

A Single-Stage High-Frequency Resonant AC/AC Converter

A PROJECT REPORT

Submitted by

KASUMARTHI DAKSESH - (111715105043)

P ADI VISHNUVARDHAN REDDY - (111715105004)

KUMAR SWAMY METTELA - (111715105048)

in partial fulfilment for the award of the degree

of

BACHELOR OF ENGINEERING

IN

ELECTRICAL AND ELECTRONICS ENGINEERING



R.M.K ENGINEERING COLLEGE, THIRUVALLUR

ANNA UNIVERSITY:: CHENNAI 600 025

APRIL 2019

BONAFIDE CERTIFICATE

Certified that this project report titled “**A SINGLE-STAGE HIGH-FREQUENCY RESONANT AC/AC CONVERTOR**” is a bonafide work of “**KASUMARTHI DAKSESH (111715105043) , PADI VISHNU VARDHAN REDDY(111715105004),KUMAR SWAMY METTELA(111715105048)**” who carried out the work under my supervision.

SIGNATURE

Dr.GEETHA RAMADAS M.E, Ph.D.

HEAD OF THE DEPARTMENT

PROFESSOR

Electrical and Electronics
R.M.K Engineering College
R.S.M. Nagar,
Kavaraipettai,
Tamil Nadu.

SIGNATURE

Mr.A.FAYAZ AHAMED M.E

SUPERVISOR

ASSISTANT PROFESSOR

Electrical and Electronics
R.M.K. Engineering College
R.S.M. Nagar,
Kavaraipettai,
Tamil Nadu.

Submitted for the Examination held on _____

INTERNAL EXAMINER

EXTERNAL EXAMINER

ACKNOWLEDGEMENT

We convey our thanks to our chairman **Thiru.R.S.Munirathinam** and vice chairman **Thiru.R.M.Kishore** who took keen interest on us and encouraged throughout the course of study and for their kind attention and valuable suggestions offered to us throughout the course of study.

We express our sincere thanks to **Dr.K.A.Mohamed Junaid**, Principal of our college for his blessings throughout our course. We take immense pleasure in thanking **Dr.Geetha Ramadas,M.E,Ph.D** Professor and Head of the Department, for having permitted us to carry out this project.

We wish to express our deep sense of gratitude to our supervisor **Mr.A.Fayaz Ahamed,M.E.**, Assistant professor, for his able guidance and useful suggestions, which helped us in completing the project work in time. We are greatly thankful to our project coordinator **Dr.T.Magesh,M.E,Ph.D.**

We are extremely grateful to all teaching faculty members of Electrical and Electronics Engineering for teaching us the importance of self-learning and the essence of keeping our self with emerging technology. Finally, yet importantly, we would like to express our heartfelt thanks to our beloved parents for their blessings, our friends, for their help and wishes for the successful completion of the project.

ABSTRACT

In many applications, such as large-scale LCD panel backlighting, street lighting, tunnel lighting, etc., an ac/dc light emitting diode (LED) driver should realize the following three functions at least: power factor correction, multichannel constant current outputs, and galvanic isolation. A novel two-stage multichannel constant current ac/dc LED driver with a low cost and simple structure is implemented, which is composed of a high-frequency resonant ac/ac converter and as many passive LCL-T resonant rectifiers as the number of the output channels. The high frequency resonant ac/ac converter is focused on in this project, which converts the ac-line input voltage into high frequency sinusoidal output voltage. First, topology derivation of the single stage high-frequency resonant ac/ac converter is presented, also the operating principle of it. Then, the steady-state performance of it is completely analyzed, including its input power factor, voltage gain, total harmonic distortion of its output voltage, and its soft switching condition. Finally, a prototype is built and the experimental results are given to verify the theoretical analysis.

List of figures

| FIGURE NO | FIGURE NAME | PAGE NO |
|-----------|--|---------|
| 1.1 | Three stage LED drive | 4 |
| 3.1 | Working model of mode 1 operation | 7 |
| 3.2 | Working model of mode 2 operation | 7 |
| 3.3 | Working model of mode 3 operation | 8 |
| 3.4 | Working model of mode 4 operation | 8 |
| 3.5 | Working model of mode 5 operation | 9 |
| 3.6 | Working model of mode 6 operation | 9 |
| 3.7 | Working model of mode 7 operation | 10 |
| 4.1 | Circuit diagram of simulation | 11 |
| 4.2 | Wave form of input voltage | 12 |
| 4.3 | Wave form of voltage in switch S_r | 13 |
| 4.4 | Wave form of current in switch S_r | 13 |
| 4.5 | Wave form of voltage in switch S_f | 13 |
| 4.6 | Wave form of current in switch S_f | 14 |
| 4.7 | Wave form of output voltage | 14 |
| 4.8 | Wave form of output power | 15 |
| 5.1 | Hardware of a single stage high frequency resonant ac/ac conveter | 16 |
| 5.2 | Output of a single stage high frequency resonant ac/ac conveter | 17 |

| FIGURE NO | FIGURE NAME | PAGE NO |
|------------------|---|----------------|
| 5.3 | Working process of Buck-Boost converter | 18 |
| 5.4 | Circuit diagram of a Crystal Oscillator | 19 |
| 5.5 | Block diagram of microcontroller | 21 |
| 5.6 | Architecture of Harvard and Von-neumann | 22 |
| 5.7 | Pin diagram of PIC16F877A | 23 |
| 5.8 | Block diagram of A/D converter | 23 |
| 5.9 | Pin diagram of TL250 Opto Coupler | 24 |
| 5.10 | Circuit of TLP250 at low side MOSFET drive | 26 |
| 5.11 | Circuit of TLP250 at high side MOSFET drive | 27 |
| 5.12 | Waveform of hardware output voltage | 27 |
| 5.13 | Waveform of triggering pulse of switch | 28 |
| 5.14 | Waveform of output voltage across switch | 28 |

LIST OF TABLES

| | | |
|-----|--|----|
| 5.1 | Resonance ranges of Crystal Oscillator | 19 |
|-----|--|----|

TABLE OF CONTENT

| CHAPTER NO | TITLE | PAGE NO |
|-------------------|--|----------------|
| | ABSTRACT | iv |
| | LIST OF FIGURES | v |
| | LIST OF TABLES | vi |
| 1 | INTRODUCTION | 1 |
| | 1.1 OVERVIEW | 1 |
| | 1.2 BLOCK DIAGRAM | 4 |
| 2 | LITERATURE SURVEY | 5 |
| 3 | OPERATION OF A SINGLE STAGE HIGH FREQUENCY RESONANT AC/AC CONVETER | 7 |
| 4 | SIMULATION | 11 |
| | 4.1 SIMULATION VALUES | 12 |
| | 4.2 SIMULATION WAVE FORMS | 12 |
| 5 | HARDWARE | 16 |
| | 5.1 HARDWARE OUTPUT | 17 |
| | 5.2 HARDWARE COMPONENTS | 18 |
| | 5.2.1 BUCK-BOOST CONVERTER | 18 |
| | 5.2.2 CRYSTEAL OSCILLATOR | 18 |
| | 5.2.3 INDUCTOR | 19 |
| | 5.2.4 MOSFET | 19 |
| | 5.2.5 LIGHT EMITTING DIODE | 20 |
| | 5.2.6 MICROCONTROLLER | 21 |

| CHAPTER NO | TITLE | PAGE NO |
|-------------------|---------------------------------------|----------------|
| | 5.2.7 OPTO COUPLER | 24 |
| | 5.2.8 OUTPUT WAVEFORMS OF HARDWARE | 27 |
| 6 | 6.1 CONCLUSION | 29 |
| | 6.2 FUTURE SCOPE | 29 |
| 7 | REFERENCES | 30 |

Chapter 1

INTRODUCTION

1.1 OVERVIEW

LIGHT-EMITTING-DIODE (LED) has become increasingly common in our daily lives for its high luminous efficacy, long lifetime, etc.. The features of high luminous efficacy and long life make it use particularly attractive in applications such as street lighting, where costs associated with system maintenance and power consumption could be greatly decreased . Commonly, input power for commercial LED street lamps lies between 60 and 240 W therefore, their drivers must employ power factor correction (PFC) techniques to achieve a high power factor to meet relevant harmonic standards, e.g., IEC 61000-3-2 . Due to packaging technology and thermal management, connecting series LED strings in parallel has been a common practice to obtain sufficient luminance. Because of the exponential voltage–current characteristic and the negative temperature coefficient of the forward voltage drop of LEDs, the current sharing ability is poor in these strings. Thus, current balancing technique is needed for the driver . Additionally, galvanic isolation is always necessary for safety consideration. All in all, an ac/dc driver for LED street lamps should realize the following three functions at least, which are PFC, multichannel constant current outputs, and galvanic isolation . Traditional three-stage multichannel constant current ac/dc LED driver for LED street lamps is shown in. High power factor is realized by the first PFC stage, and the ac input voltage is converted into stable dc-link voltage. The second front-end dc/dc converter stage is in the charge of providing galvanic isolation and converting the dc-link voltage into lower output dc voltage, moreover, the low-frequency voltage ripple of the dc-link voltage is greatly reduced. The third stage named constant current source stage makes the current through each LED string constant and current balancing among all LED strings is achieved. Since galvanic isolation is realized by employing a high-frequency isolation

transformer in the second front-end dc/dc stage, a dc/ac unit and an ac/dc unit are included. Therefore, in spite of its good performance, this three-stage solution is complicated and its efficiency is lowered to some extent; moreover, for the third stage to provide multiple constant current sources, each LED constant current source has its own power stage and controller, which increases the cost.

In order to simplify the circuit structure, boost efficiency, and reduce cost, many two-stage solutions are proposed by integrating the front-end dc/dc stage and constant current source stage into a second multichannel constant current source stage, as shown in . In a multichannel constant current source is constructed by as many asymmetrical half bridges (AHBs) as LED strings. All the AHBs are galvanic isolated and the output current of each AHB is regulated to supply the LED string with constant current, since AHB can achieve soft switching in primary switches and high efficiency is achieved. However, the structure is still complicated and the cost is high because each AHB has its own power stage and controller. In an LLC resonant converter with multitransformer and voltage doubler configuration is adopted to serve as a multichannel constant current source. Because of the series connection of the primary side windings of the transformers and the charge balancing of the dc block capacitors, all output currents are automatically balanced. The structure is simplified and the cost is reduced when compared with the solution in , however, in order to implement a $2n$ -channels constant current source, n separated transformers are needed. In a multichannel constant current source with only one transformer is proposed based on charge balancing principle of the dc block capacitors. The structure is further simplified and the cost is further reduced, thus it is a competitive solution. In a multichannel constant current source with dynamic sinusoidal bus voltage regulation is proposed, which is composed of an *LCLC* series–parallel resonant inverter and as many passive LCL-T resonant

rectifiers as output channels. It is a modular solution and can achieve multichannel constant current outputs as needed conveniently.

Inspired by this point that the passive LCL-T resonant rectifier analyzed in can achieve constant output current without any control circuits provided that the amplitude of its input sinusoidal voltage is regulated to a constant value and the frequency of it is equal to the resonant frequency of the LCL-T resonant tank, another two-stage multichannel constant current ac/dc LED driver shown In is proposed, which is composed of a high frequency resonant ac/ac converter and as many passive LCL-T resonant rectifiers as the number of the LED strings needed. The high-frequency resonant ac/ac converter converts the ac-line voltage into high-frequency sinusoidal voltage with fixed amplitude and frequency, and implements PFC and galvanic isolation. The passive resonant rectifiers achieve multichannel constant current outputs inherently, since the resonant frequency of the LCL-T resonant network is equal to the frequency of its input sinusoidal voltage. The main advantage of the proposed two-stage solution is that it is a modular and cheap solution to realize multichannel outputs since only a passive resonant rectifier is needed to increase a constant current output channel, and only eight passive components are included to build a LCL-T resonant rectifier. The main disadvantage is that the output current of each output channel is not closed-loop regulated and the accuracy of it is affected by the tolerance of the passive components. The influence of the component tolerance on the output current is evaluated in and it is possible to make the current difference among the output channels within 5% with proper design according to the experimental results. Since the passive LCL-T resonant rectifier has been completely analyzed in the main focus of this paper is the front high-frequency resonant ac/ac converter. There are two cascaded power conversion units included in the high-frequency resonant ac/ac converter, which are PFC unit and high-frequency resonant dc/ac unit. If the two units are independent, which means each unit has its own power stage and

controller, the converter is called two-stage high-frequency resonant ac/ac converter. The two-stage solution has good performance, however, the component count is large and the cost is high, which can be used for high power applications. For the low-to-medium power applications, such as LED driver, single-stage solution is preferred because the component count and the cost can be obviously reduced by sharing the switches of the two power conversion units and adopting only one controller. In a low-frequency ac to high-frequency ac inverter is presented, the cost is reduced when compared with the two-stage solution because only one unified controller is employed. However, the power stage of the inner two power conversion units is independent. In this paper, a true single-stage high-frequency resonant ac/ac converter is proposed by integrating the PFC unit and high-frequency resonant dc/ac unit into one power stage and adopting only one controller, thus the component count and cost are reduced further.

This paper is organized as follows. In Section II, the topology derivation of the single-stage high-frequency resonant ac/ac converter is described. The operating principle of the converter is presented in Section III and the performance of it is analyzed in Section IV in detail. The experimental results are given in Section IV and Section V summarizes the conclusions drawn from the investigation.

1.2 BLOCK DIAGRAM

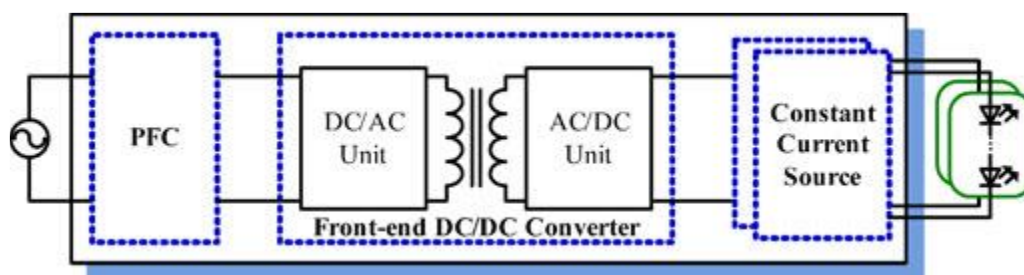


Figure1.1: Three stage LED drive

CHAPTER 2

LITERATURE SURVEY

Duan and **Jin** from University of British Columbia made a thorough evaluation of different digital control design methods for DC-DC converters . The methods include direct and indirect design approaches. In the direct design approach, small signal models of the converters are first converted into discrete-time models, and digital controllers are directly designed based on the discrete-time models. In the indirect design approach, analog controllers are first designed based on the small signal models of the converters, and then converted into digital controllers. The best approach is determined based on a comparison of experimental results. It was concluded that the direct design approach is better than an indirect design approach. Backward integration methods were suggested to be a better discretization method for the indirect design approach.

Bibian and **Jin** from the University of British Columbia studied two prediction techniques for the compensation of digital control time delay in DC-DC converters. Modified predictor and simplified predictor were developed to increase the bandwidth of the control loop . **Vallittu, Suntio and Ovaska** studied the opportunities and 16 constraints of digital control of power supplies. The advantages and disadvantages of analog and digital control of power supplies were compared in .

D. Jeff Shorttetal, proposed an unconventional switched mode power supply (SMPS) architecture, developed as four 150-W buck-boost or fly back-type switching stages operated in phase-shifted-parallel. The fly backs are operated in the continuous mode with intersecting conduction on both input and output sides; they are switched in cyclic sequence with one-fourth of a switching period following turn ON of one stage before turn ON of the next stage. This method reduces the effective input and output ripple currents of the DC-DC converter because the frequency was N (N is the number of parallel

stages) times the switching frequency of one stage, and the power stage ripple current was dramatically less than a comparable converter.

In 1990 **K. Mahabir** et al focused on designing of control schemes for high power factor AC to DC converters using a boost converter whose input voltage $V_{in}(t)$ is the rectified AC waveform and introduced a new linear model for high power factor AC to DC converters. Time invariant or periodically varying controllers, acting at the time scales of the line or switching periods respectively, can then be designed from the resulting averaged or sampled data models. The designing and the selection of the boost inductor and circuit performances were developed and verified with measurements by Chen Zhou et al. A computer aided design program was developed to select the optimal circuit components. Design guidelines for the low frequency feedback network were presented using the switch model for the power factor correction circuit. Small-signal transfer functions for open and closed-loop responses were derived.

Later on, the research was being carried out in reducing the switching losses, power losses, reduction in the weight of the converter and power factor correction methods. Richard Redl and Nathan O.Sokal proposed a novel soft switching method for DC-DC converter. The converter adds up an external commutating inductor and two clamp diodes to the phase-shifted PWM full-bridge DC-DC converter substantially reduces the switching losses of the transistors and the rectifier diodes, under all loading conditions. The addition of these elements also eliminates the overshoot and ringing of the rectifier diodes associated with their charge storage and junction capacitances. The commutating inductance also helps to ensure lossless 17 transition of the converter, without requiring excessive magnetizing current in the transformer .

Chapter 3

OPERATION OF A SINGLE-STAGE HIGH-FREQUENCY RESONANT AC/AC CONVERTER

The analysis and descriptions for every operating mode are listed as follows.

Mode 1 :

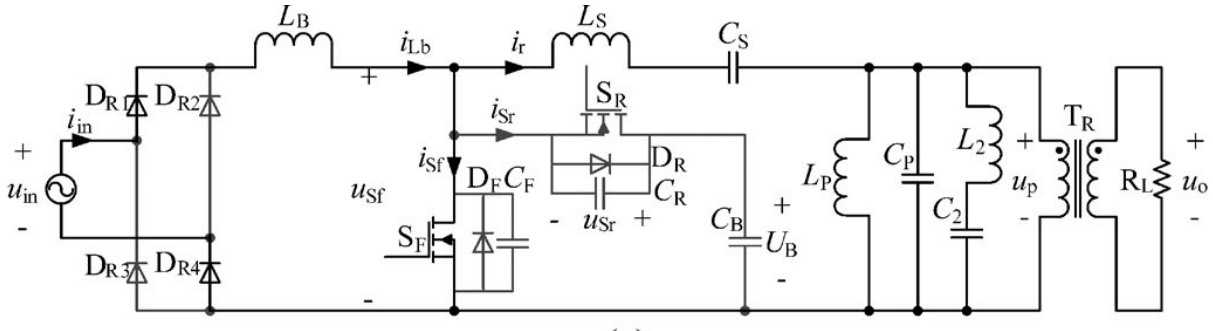


Figure 3.1: Working model of mode 1 operation

Figure 3.1 shows the working operation of mode 1. At t_0 , S_F is turned ON with zero voltage since the intrinsic diode is forced to conduct in the previous mode. The inductor current i_{Lb} increases linearly, simultaneously, the energy stored in the resonant tank freewheels through switch S_F and keeps supplying power to the load.

Mode 2 :

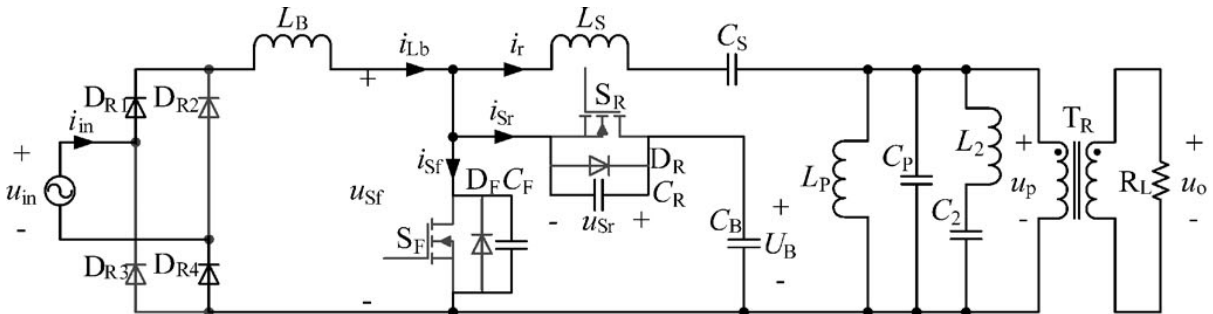


Figure 3.2: Working model of mode 2 operation

Figure 3.2 shows the working operation of mode 2. At t_1 , SF is turned OFF, CF is charged, and CR is discharged at the same time. Since the increase rate of u_{Sf} is limited by CF and CR, SF is turned OFF at ZVS approximately and the turn-OFF losses of it can be reduced. Once u_{Sf} increases to U_B and u_{Sr} decreases to zero, this mode ends.

Mode 3 :

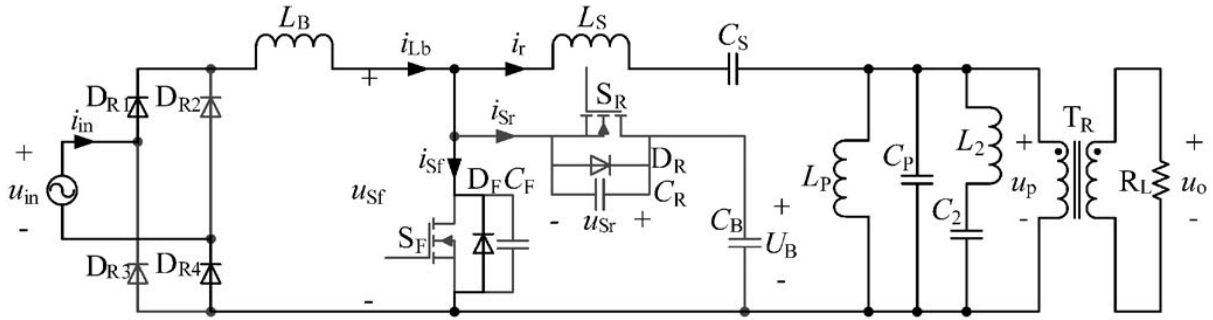


Figure 3.3: Working model of mode 3 operation

Figure 3.3 shows the working operation of mode 3. At t_2 , u_{Sr} decreases to zero and the intrinsic diode DR is forced to conduct. During this mode, L_B is discharged by $u_{in} - U_B$, and the energy stored in it releases to C_B and the resonant tank.

Mode 4 :

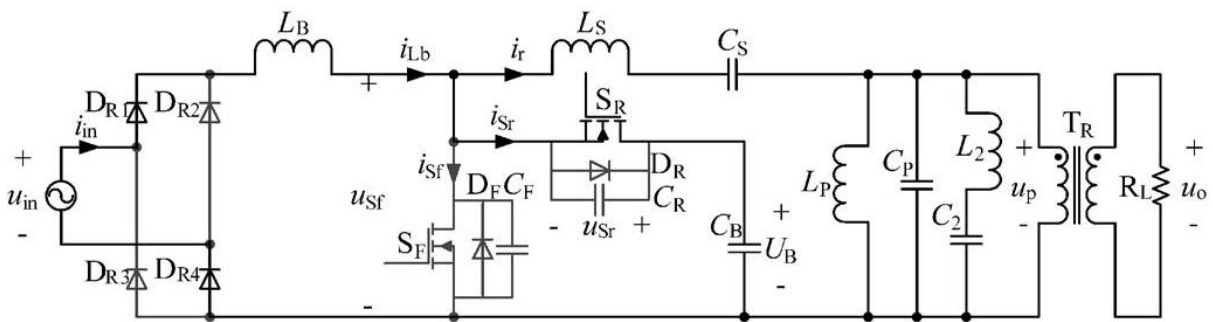


Figure 3.4: Working model of mode 4 operation

Figure 3.4 shows the working operation of mode 4. At t_3 , SR is gated ON at ZVS because u_{Sr} is clamped to zero by the DR. In this mode, the equivalent circuit is similar to mode 3.

Mode 5 :

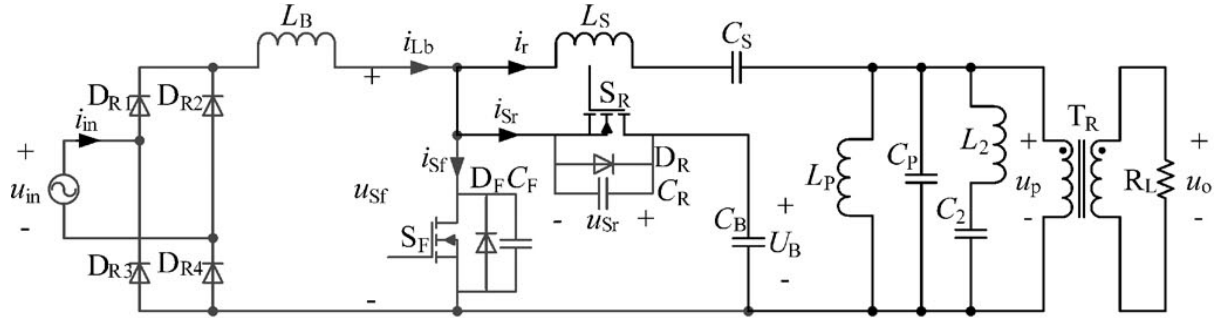


Figure 3.5: Working model of mode 5 operation

Figure 3.5 shows the working operation of mode 5 . At t_4 , inductor current i_{Lb} decreases to zero, simultaneously, diodes DR1 and DR2 are reverse biased. In this mode, the energy stored in CB releases to the resonant tank and keeps supplying power to the load.

Mode 6 :

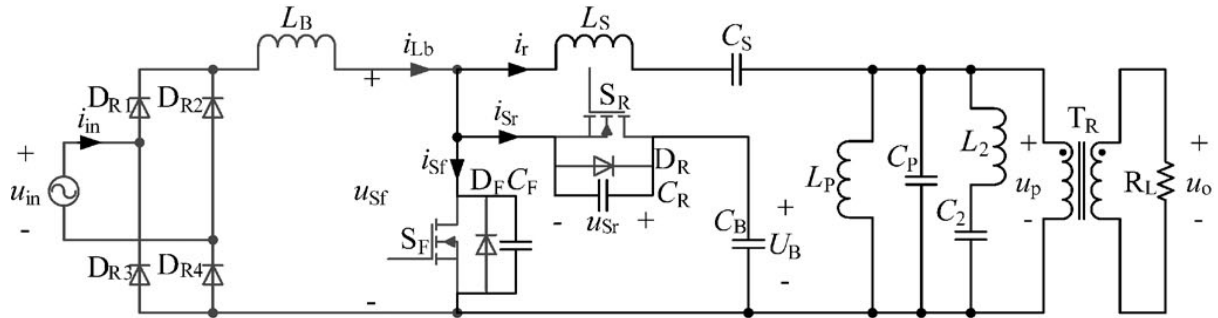


Figure 3.6: Working model of mode 6 operation

Figure 3.6 shows the working operation of mode 6. At t_5 , SR is turned OFF. Similarly, the increase rate of u_{Sr} is limited by CF and CR, SR is turned OFF at ZVS approximately and its turn-OFF losses are reduced.

Mode 7 :

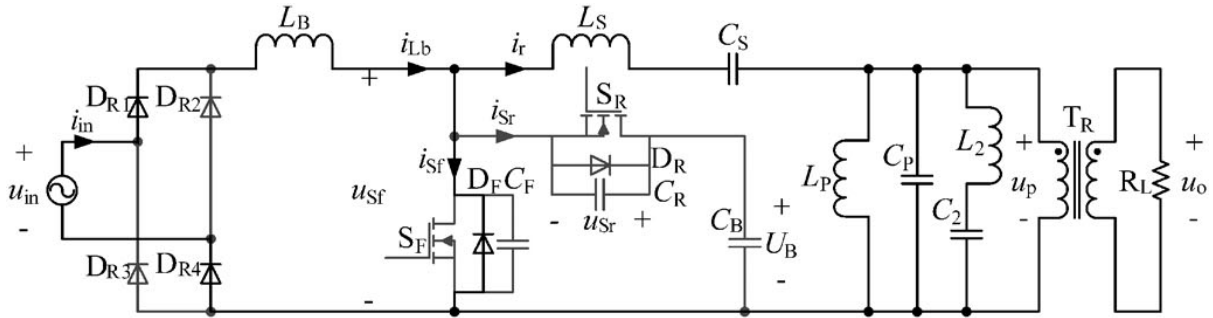


Figure 3.7: Working model of mode 7 operation

Figure 3.7 shows the working operation of mode 7. At t_6 , u_{Sf} decreases to zero and the intrinsic diode DF starts to conduct, which creates a ZVS condition for turning ON SF. In this mode, diodes DR1 and DR4 are forced to conduct, the boost inductor L_B is charged by the ac-line voltage u_{in} . At t_7 , SF is turned ON at ZVS and the converter begins a new switching cycle.

The above performed operational modes are for the positive half-cycle. The operational modes of negative half-cycle is as same as positive half-cycle.

Chapter 4

SIMULATION

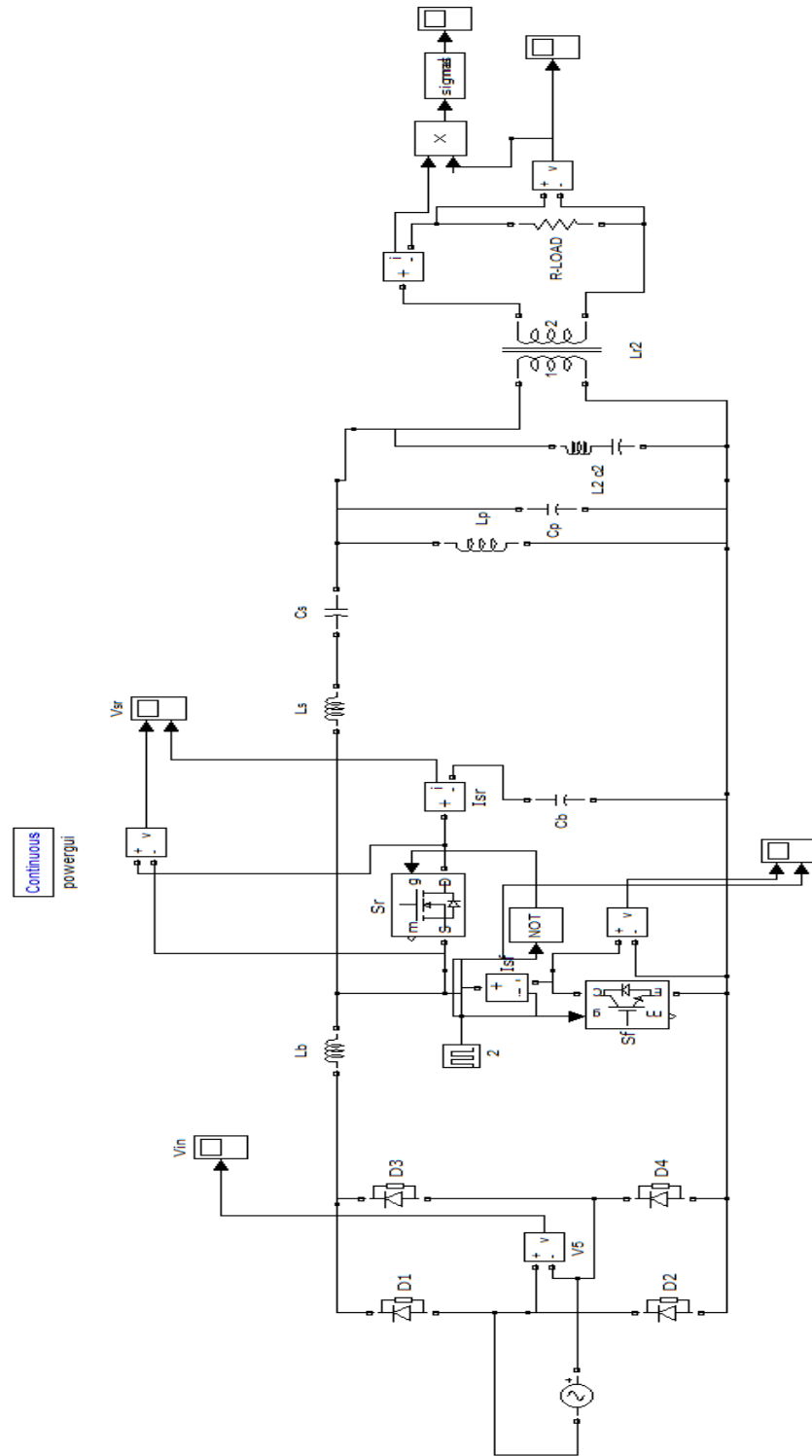


Figure 4.1 : Circuit diagram of simulation

4.1 STIMULATION VALUES:

Input voltage: $u_{in} = 220 \text{ Vac}/50 \text{ Hz}$ •

Output voltage: $u_o = 45 \text{ Vac}/100 \text{ kHz}$;

Output power: $P_o = 130 \text{ W}$;

Switching frequency: $f_{SW} = 100 \text{ kHz}$.

Duty cycle $D=0.16$.

$L_s=108.99\mu\text{H}$ $L_p=21.61 \mu\text{H}$.

$C_s=28.69\text{nF}$ $C_p=0.08 \mu\text{F}$.

$L_2=83.39 \mu\text{H}$ $C_2=7.59\text{nF}$.

$K_{sr}=0.9$. $K_{pr}=2.5$.

$Q_{sr}=2.5$. $Q_2=2.0$.

4.2 Simulation wave form

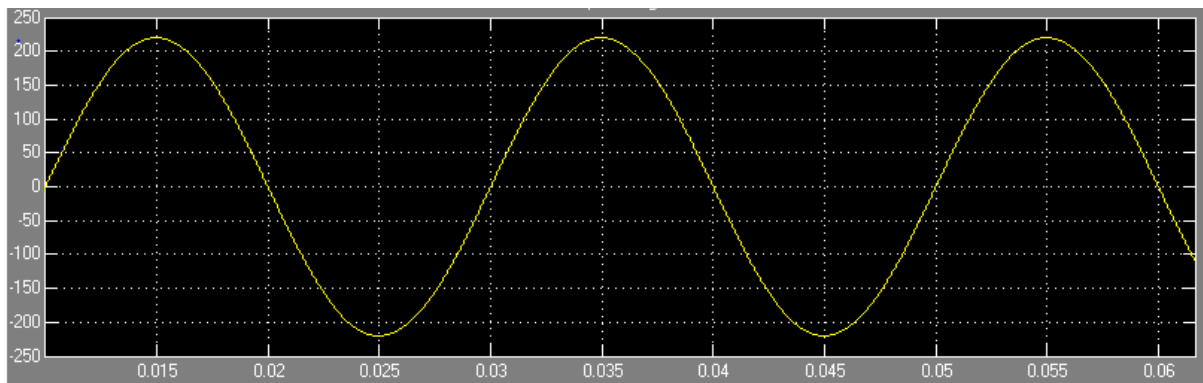


Figure 4.2:wave form of input voltage.

The figure 4.2 shows the wave form of input voltage given to the resonant converters.

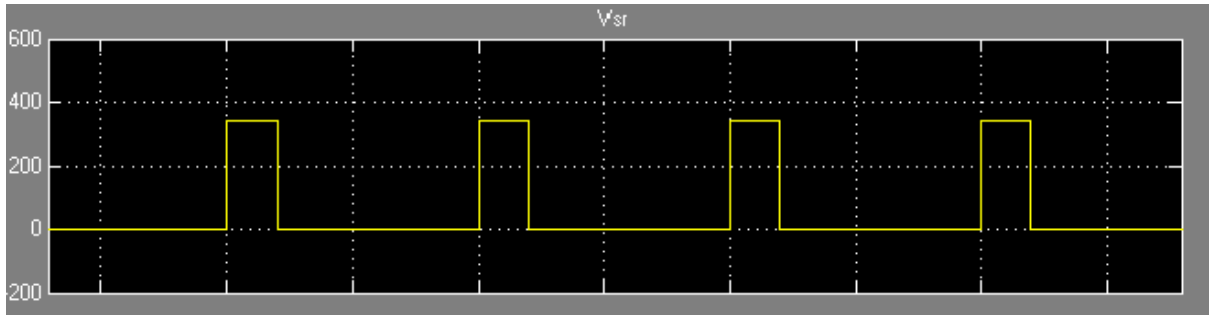


Figure 4.3: wave form of voltage in switch S_r .

The figure 4.3 shows the wave form representing the voltage across the switch S_r .

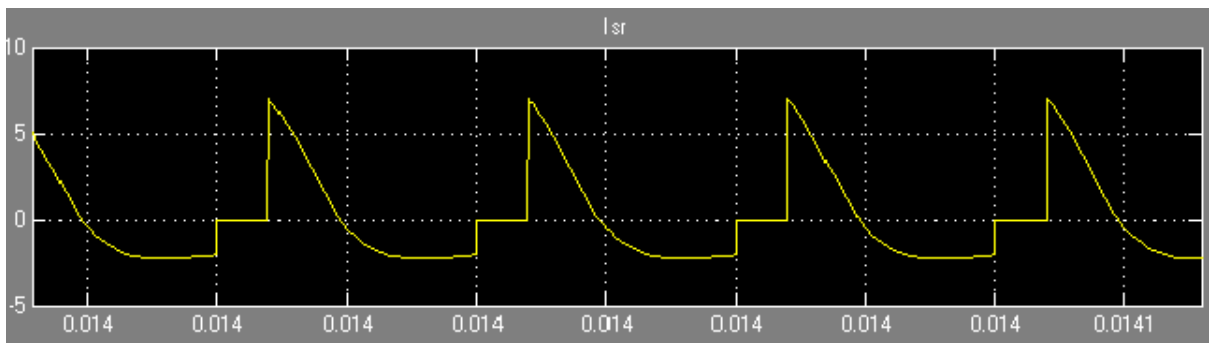


Figure 4.4: wave form of current in switch S_r .

The figure 4.4 shows the wave form representing the current in switch S_r .

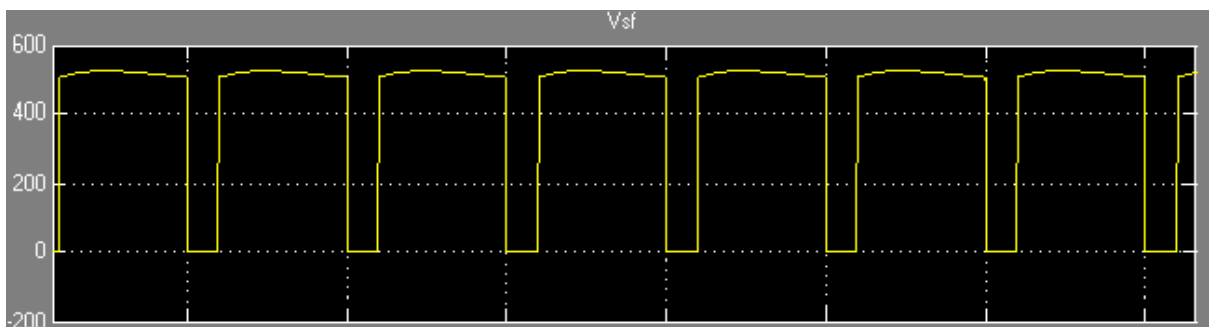


Figure 4.5: wave form of voltage in switch S_f .

The figure 4.5 shows the wave form representing the voltage across the switch S_f .

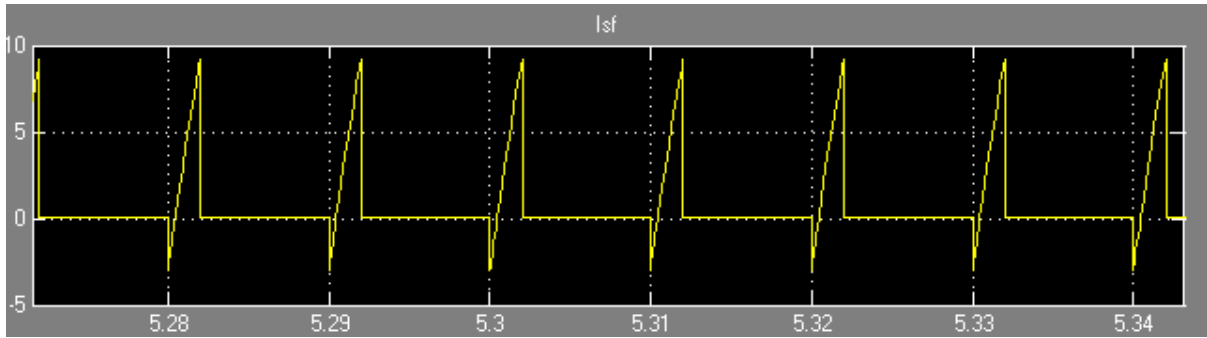


Figure 4.6: wave form of current in switch S_f .

Figure 4.6 shows the wave form representing the current in the switch S_f .

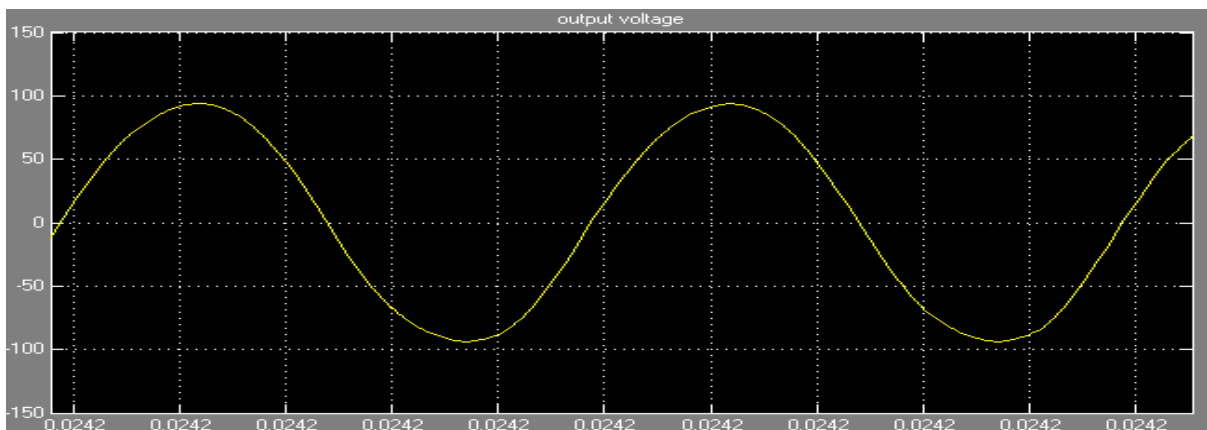


Figure 4.7: wave form of output voltage

The Figure 4.7 shows the wave form representing the output voltage .

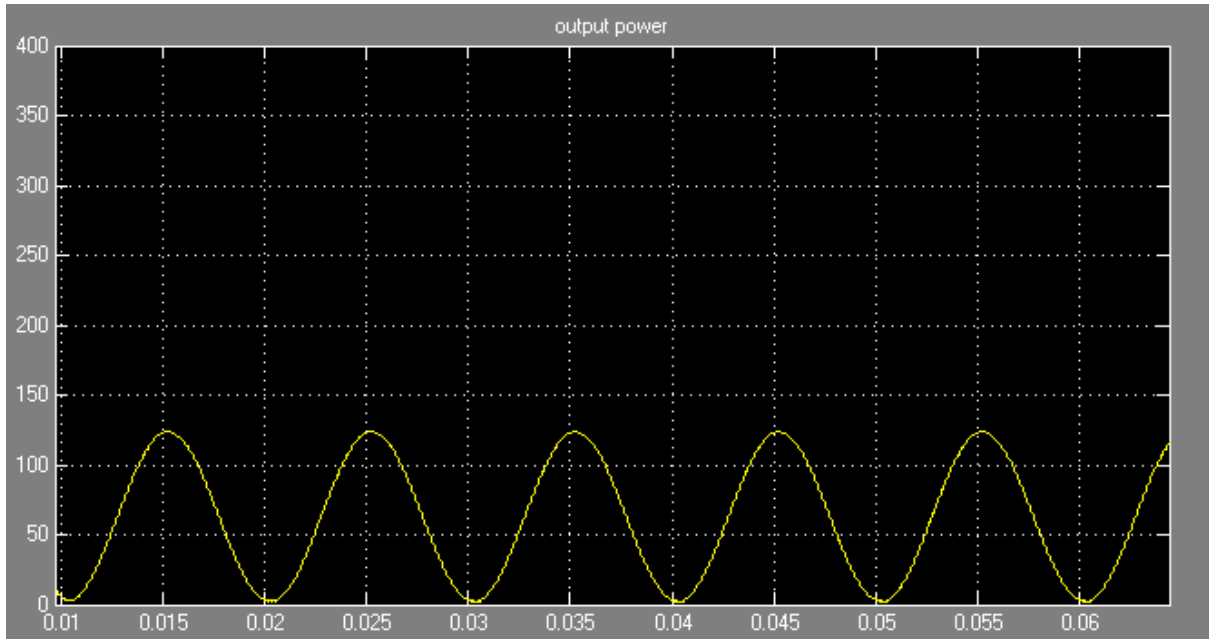


Figure 4.8: wave form of output power.

The figure 4.8 shows the wave form of output power of the simulation .

Chapter 5

HARDWARE

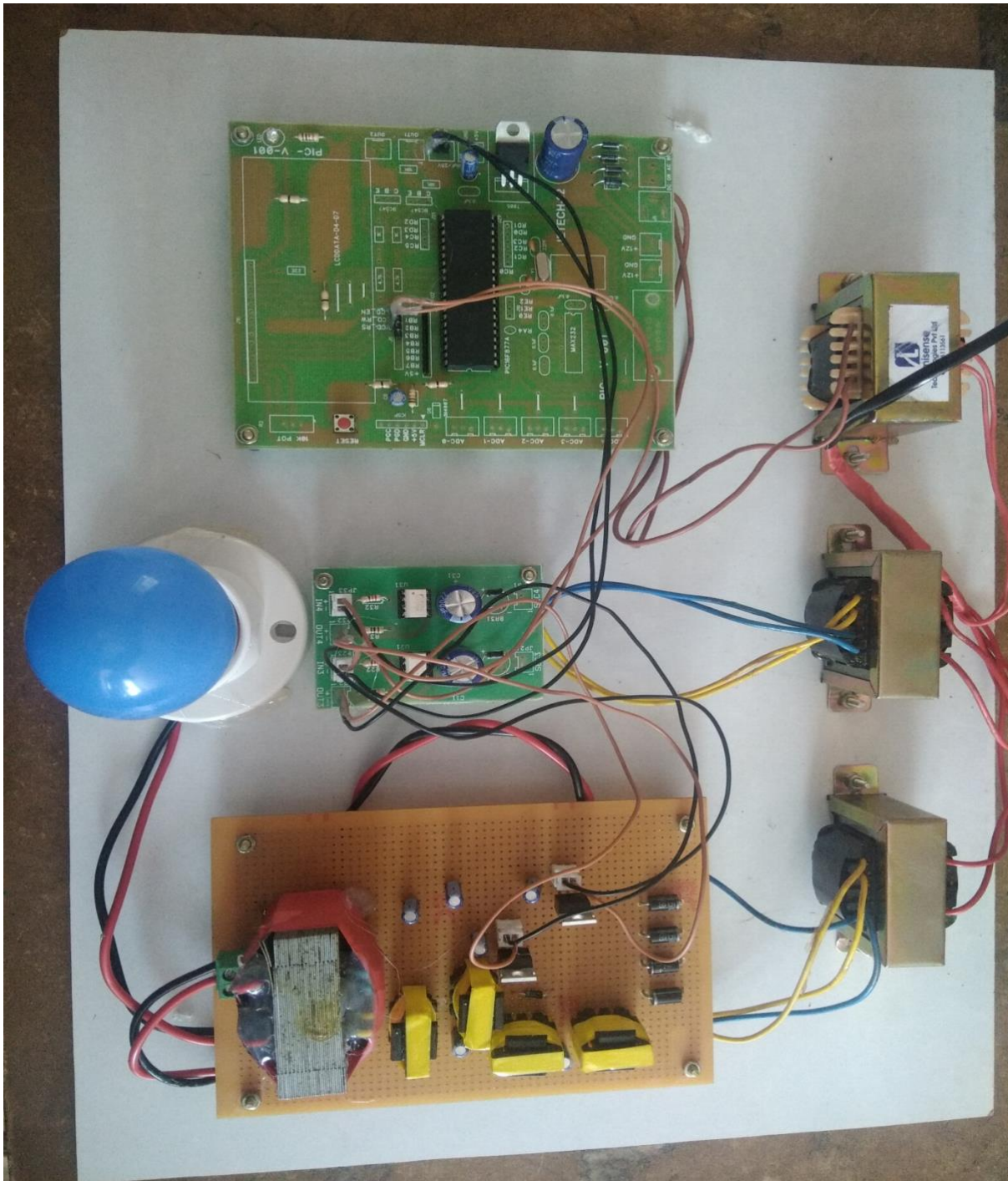


FIGURE 5.1 : HARDWARE OF A SINGLE-STAGE HIGH-FREQUENCY RESONANT AC/AC CONVERTER

CHAPTER 5.1 HARD WARE OUTPUT

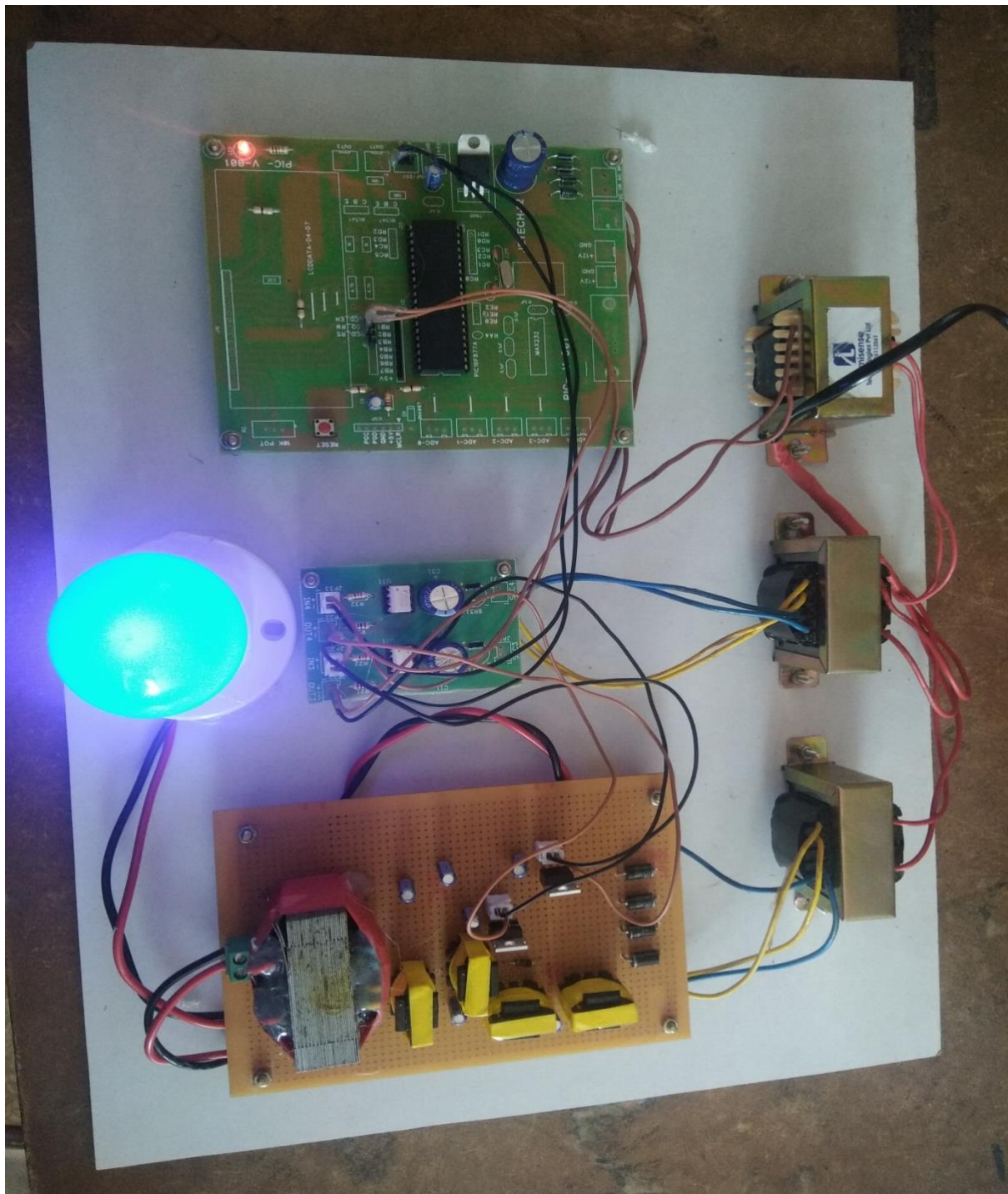


FIGURE 5.2 : OUTPUT OF A SINGLE-STAGE HIGH-FREQUENCY
RESONANT AC/AC CONVERTER

5.2 COMPONENTS USED IN HARDWARE:

5.2.1 BUCK-BOOST CONVERTER:

The Buck–boost converter is a type of DC-DC converter that has an output voltage magnitude that is either greater than or less than the input voltage magnitude. It is a switch mode power supply with a similar circuit topology to the boost converter and the buck converter. The output voltage is adjustable based on the duty cycle of the switching transistor. One possible drawback of this converter is that the switch does not have a terminal at ground; this complicates the driving circuitry. Also, the polarity of the output voltage is opposite the input voltage. Neither drawback is of any consequence if the power supply is isolated from the load circuit (if, for example, the supply is a battery) as the supply and diode polarity can simply be reversed. The switch can be on either the ground side or the supply side.

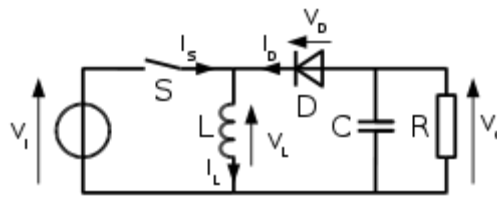


Figure 5.3: Working process of a Buck-Boost converter

5.2.2 CRYSTAL OSCILLATOR:

A crystal oscillator is an electronic circuit that uses the mechanical resonance of a vibrating crystal of piezoelectric material to create an electrical signal with a very precise frequency. This frequency is commonly used to keep track of time (as in quartz wristwatches), to provide a stable clock signal for digital integrated circuits, and to stabilize frequencies for radio transmitters/receivers

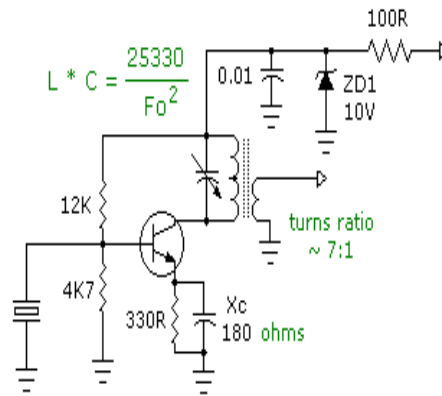


Figure 5.4:circuit diagram of a Crystal Oscillator

CERAMIC RESONATORS

| Ranges Tested: | | | |
|---|------------------------|-----------|-----------|
| Mode | Freq. | OSC1 | OSC2 |
| XT | 455 kHz | 68-100 pF | 68-100 pF |
| | 2.0 MHz | 15-68 pF | 15-68 pF |
| | 4.0 MHz | 15-68 pF | 15-68 pF |
| HS | 8.0 MHz | 10-68 pF | 10-68 pF |
| | 16.0 MHz | 10-22 pF | 10-22 pF |
| These values are for design guidance only. See notes following Table 14-2. | | | |
| Resonators Used: | | | |
| 2.0 MHz | Murata Erie CSA2.00MG | ± 0.5% | |
| 4.0 MHz | Murata Erie CSA4.00MG | ± 0.5% | |
| 8.0 MHz | Murata Erie CSA8.00MT | ± 0.5% | |
| 16.0 MHz | Murata Erie CSA16.00MX | ± 0.5% | |
| All resonators used did not have built-in capacitors. | | | |

Table 5.1:Resonance ranges of Crystal Oscillator

5.2.3 INDUCTOR:

An inductor, also called a coil or reactor, is a passive two-terminal electrical component which resists changes in electric current passing through it. It consists of a conductor such as a wire, usually wound into a coil. Energy is

stored in a magnetic field in the coil as long as current flows. When the current flowing through an inductor changes, the time-varying magnetic field induces a voltage in the conductor, according to Faraday's law of electromagnetic induction. According to Lenz's law the direction of induced electromotive force is always such that it opposes the change in current that created it. As a result, inductors always oppose a change in current, in the same way that a flywheel opposes a change in rotational velocity. Care should be taken not to confuse this with the resistance provided by a resistor

5.2.4 MOSFET:

This N-Channel enhancement mode silicon gate power field effect transistor is an advanced power MOSFET designed, tested, and guaranteed to withstand a specified level of energy in the breakdown avalanche mode of operation. All of these power MOSFETs are designed for applications such as switching regulators, switching converters, motor drivers, relay drivers, and drivers for high power bipolar switching transistors requiring high speed and low gate drive power. These types can be operated directly from integrated.

Details: 8A, 500V, 0.850 Ohm, N-Channel Power.

Product no:IRF840.

5.2.5 LIGHT-EMITTING DIODE:

A light-emitting diode (LED) is a two-lead semiconductor light source . It is a pn-junction diode , which emits light when activated. When a suitable voltage is applied to the leads, electrons are able to recombine with electron holes within the device, releasing energy in the form of photons . This effect is called electroluminescence , and the color of the light is determined by the energy band gap of the semiconductor.

5.2.6 MICROCONTROLLER:

Circumstances that we find ourselves in today in the field of microcontrollers had their beginnings in the development of technology of integrated circuits. This development has made it possible to store hundreds of thousands of transistors into one chip. That was a prerequisite for production of microprocessors, and the first computers were made by adding external peripherals such as memory, input-output lines, timers and other. Further increasing of the volume of the package resulted in creation of integrated circuits. These integrated circuits contained both processor and peripherals. That is how the first chip containing a microcomputer, or what would later be known as a microcontroller came about.

Microcontroller with its basic elements and internal connections

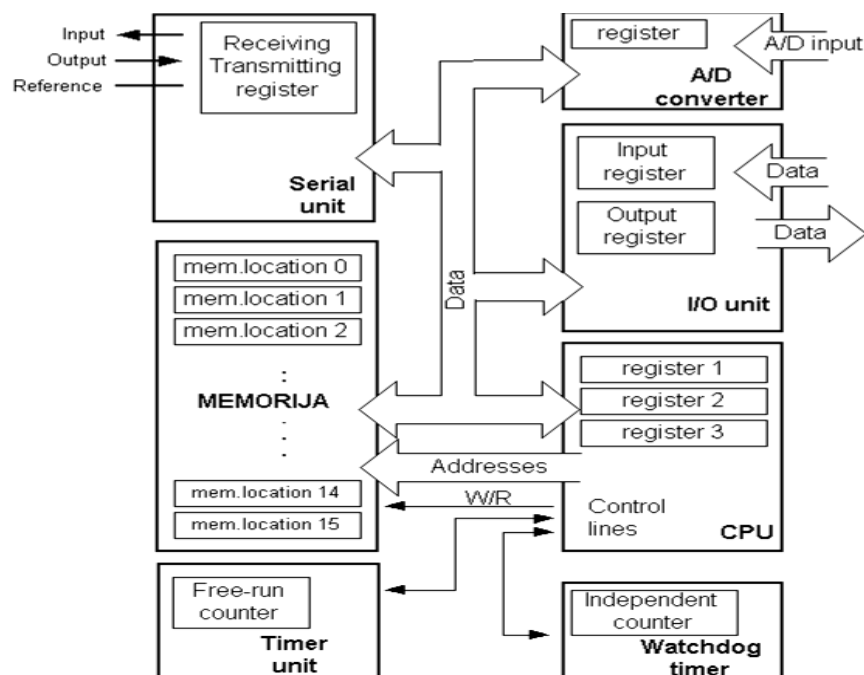


Figure 5.5:Block diagram of microonroller

CISC and RISC

Harvard architecture is a newer concept than Von-Neumann's. It rose out of the need to speed up the work of a microcontroller. In Harvard architecture, data bus and address bus are separate. Thus a greater flow of data is possible

through the central processing unit, and of course, a greater speed of work. Separating a program from data memory makes it further possible for instructions not to have to be 8-bit words. It is also typical for Harvard architecture to have fewer instructions than von-Neumann's, and to have instructions usually executed in one cycle.

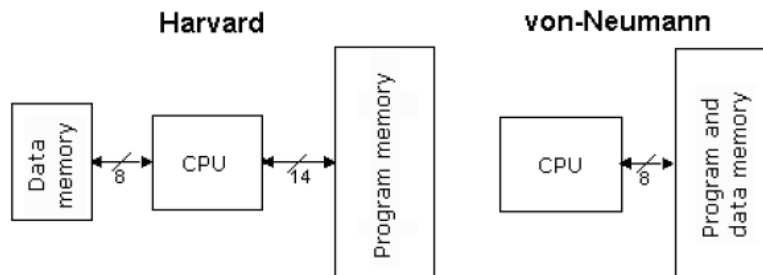


Figure 5.6:Architecture of Harvard and von-neumann

Microcontrollers with Harvard architecture are also called "RISC microcontrollers". RISC stands for Reduced Instruction Set Computer. Microcontrollers with von-Neumann's architecture are called 'CISC microcontrollers'. Title CISC stands for Complex Instruction Set Computer. Since PIC16F877 is a RISC microcontroller, that means that it has a reduced set of instructions, more precisely 35 instructions. All of these instructions are executed in one cycle except for jump and branch instructions. PIC16F877 usually reaches results of 2:1 in code compression and 4:1 in speed in relation to other 8-bit microcontrollers in its class.

Memory organization

There are three memory blocks in each of these PICmicro MCUs. The Program Memory and Data Memory have separate buses so that concurrent access can occur.

Pin layout of PIC16F877A

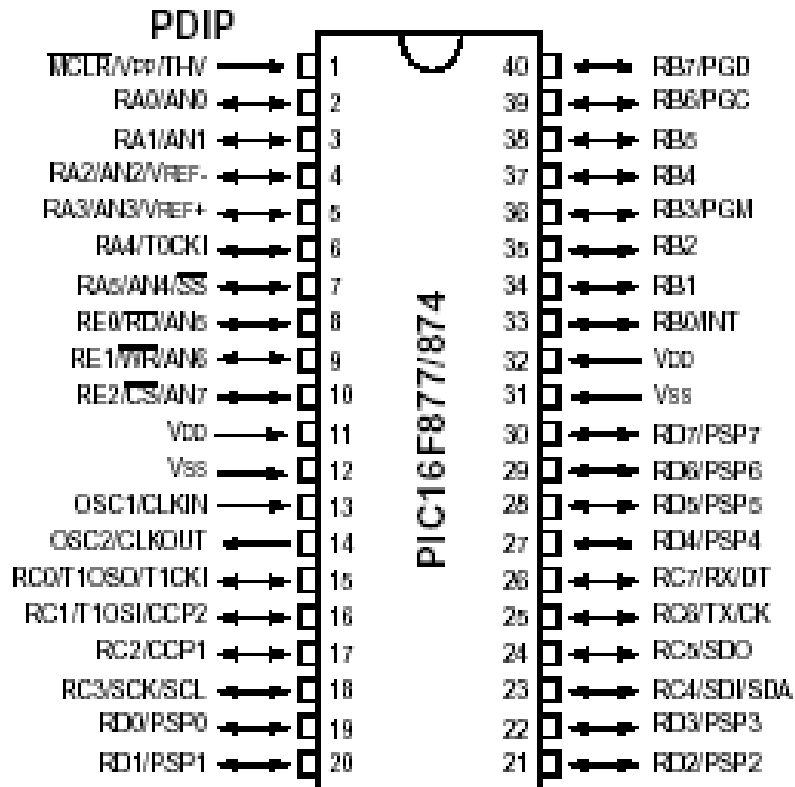


Figure 5.7: Pin diagram of PIC16F877A

Analog to Digital Converter

As the peripheral signals usually are substantially different from the ones that microcontroller can understand (zero and one), they have to be converted into a pattern which can be comprehended by a microcontroller.

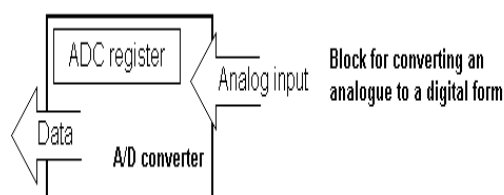


Figure 5.8: Block diagram of A/D converter

This task is performed by a block for analog to digital conversion or by an ADC. This block is responsible for converting an information about some

analog value to a binary number and for follow it through to a CPU block so that CPU block can further process it.

5.2.7 OPTOCOUPLER

Isolated MOSFET driver TLP250 working

In this article I will discuss isolated Mosfet driver TLP250. Mosfet driver TL250 like other MOSFET drivers have input stage and output stage. It also have power supply configuration. TLP250 is more suitable for MOSFET and IGBT. The main difference between TLP250 and other MOSFET drivers is that TLP250 MOSFET driver is optically isolated. Its mean input and output of TLP250 mosfet driver is isolated from each other. Its works like a optocoupler. Input stage have a light emitting diode and output stage have photo diode. Whenever input stage LED light falls on output stage photo detector diode, output becomes high.

Pin configuration isolated mosfet driver TL250

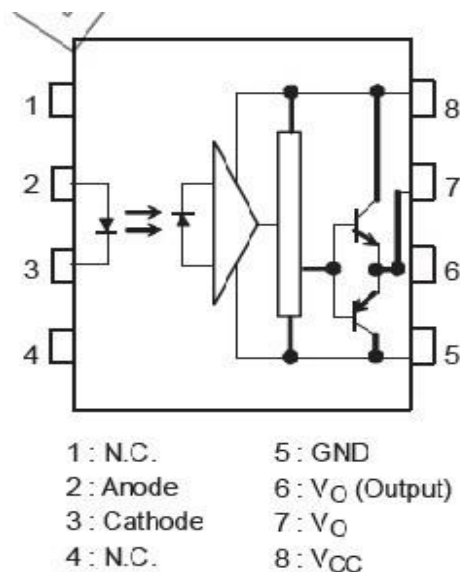


Figure 5.9: Pin Diagram of TL250 Opto Coupler.

Pin layout of TLP250 is given below. It is clearly shown in figure that led at input stage and photo detector diode at output stage is used to provide isolation between input and ouput. Pin number 1 and 4 are not connected to any point. Hence they are not in use. Pin 2 is anode point of input stage light

emitting diode and pin 3 is cathode point of input stage. Input is provided to pin number 2 and 3. Pin number 8 is for supply connection. Pin number 5 is for ground of power supply. Pin number one and four is not connected to any point physically. Therefore they are not in use.

Pin number 8 is used to provide power supply to TLP250 and pin number 5 is ground pin which provides return path to power supply ground. Maximum power supply voltage between 15-30 volt dc can be given to TLP250. But it also depends on temperature of environment in which you are using TLP250.

Pin number 2 and 3 are anode and cathode points of input stage LED. It works like a normal light emitting diode. It has similar characteristics of forward voltage and input current. Maximum input current is in the range of 7-10mA and forward voltage drop is about 0.8 volt. TLP250 provides output from low to high with minimum threshold current of 1.2mA and above.

Pin number six and seven is internally connected to each other. Output can be taken from either pin number 6 and 7. Totem pole configuration of two transistors is used in TLP250. In case of high input, output becomes high with output voltage equal to supply voltage and in case of low input, output becomes low with output voltage level equal to ground. MOSFET driver TLP250 can be used up to 25kHz frequency due to slow propagation delay. This is all about pin configuration and working of TLP250. Now I will talk about how to use isolated MOSFET driver TLP250 as low side MOSFET driver and high side MOSFET driver.

TLP250 as a low side MOSFET driver

Circuit diagram of low side MOSFET driver using TLP250 is shown below. In this circuit diagram, TLP250 is used as non-inverting low side MOSFET driver. You should connect an electrolytic capacitor of value 0.47μF between power supply. It provides protection to TLP250 by providing stabilized voltage to IC.

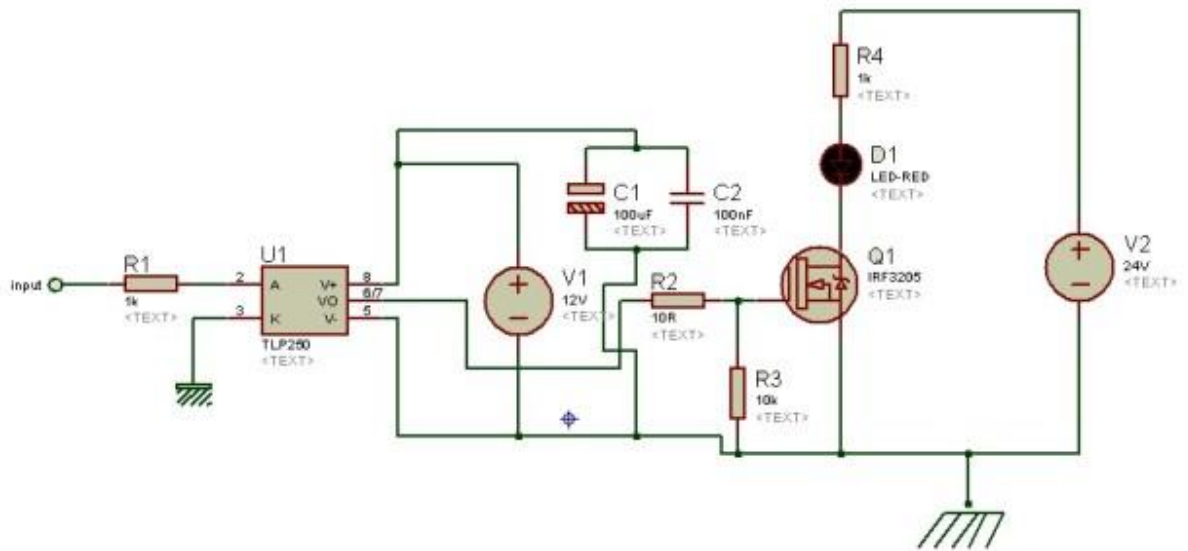


Figure 5.10: Circuit of TLP250 at low side MOSFET driver

As shown in figure above input is drive signal that drives the output. Vin is according to signal ground. It should not be connected with supply ground and output ground. It is clearly shown in above figure TLP250 and load ground is referenced to the power ground and it is isolated from input signal reference ground. When input is high, MOSFET Q1 get high signal from TLP250 and it is driven by power supply and current flows through the load. When input is low, MOSFET Q1 get low signal from TLP250 output pin and mosfet Q1 remains off and there is no current flow to load. Value of supply voltage ranges between 10-15 volt. Input resistor at gate of MOSFET is used depend on amplitude of input signal. Usually input signal is provided through microcontroller and microcontroller input signal level is in the order of 5 volt. Capacitor C1 is used as decoupling capacitor.

TLP250 as a high side MOSFET driver

Circuit diagram of MOSFT driver tlp250 used as high side driver is shown below. It is used as non inverting high side mosfet driver. Because input signal ground is connected to cathode of input stage light emitting diode. Therefore it is used as a non inverting high side mosfet driver.

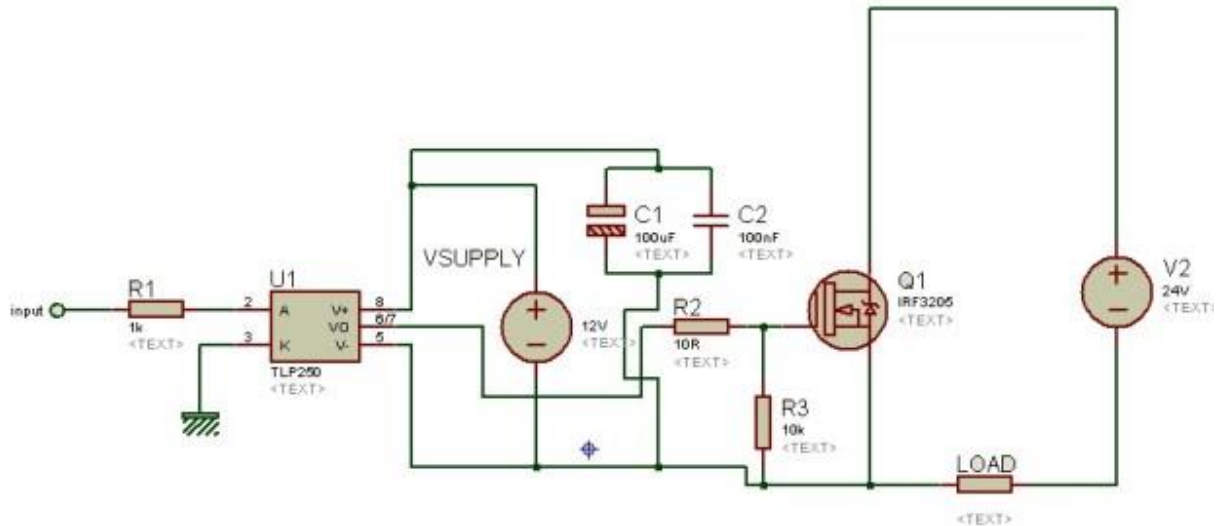


Figure 5.11: Circuit of TLP250 at high side MOSFET driver.

In high side configuration there are three grounds as shown in figure above. Ground of input signal, ground of supply voltage and ground of power supply voltage. Remember that while using TLP250 as high side MOSFET driver, all grounds should be isolated from each other.

5.2.8 Output wave forms of hardware

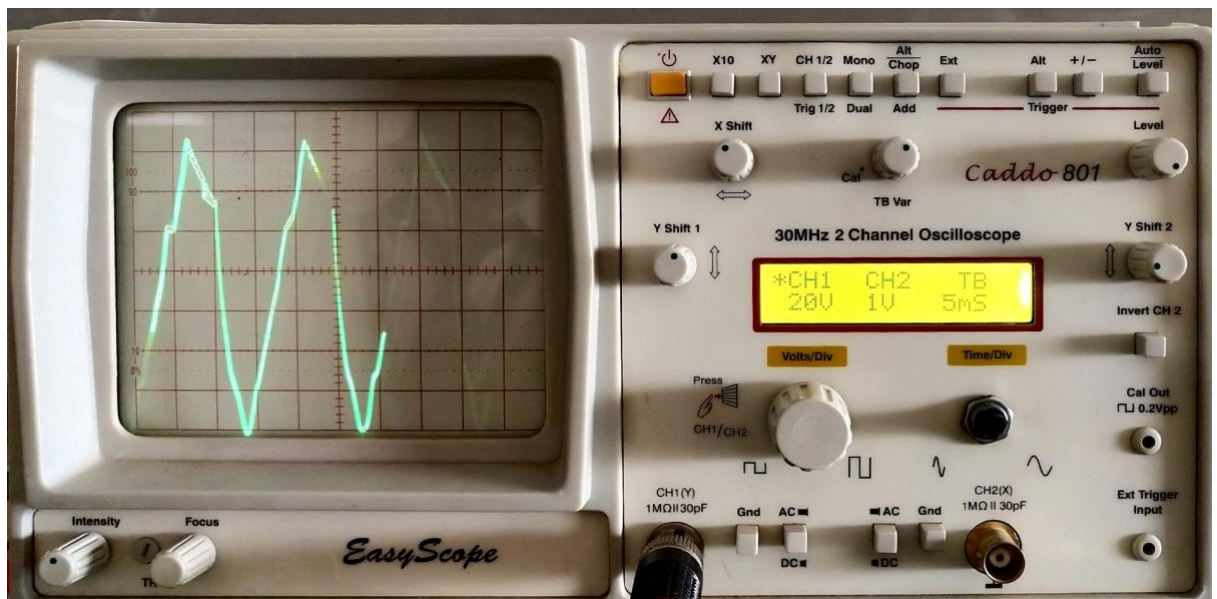


Figure 5.12:Wave form of hardware output voltage .

Figure 5.12 shows the wave form of hardware output voltage taken from a CRO. Output voltage =80v, On-Time=5.6ms,Off-Time=4.8ms.

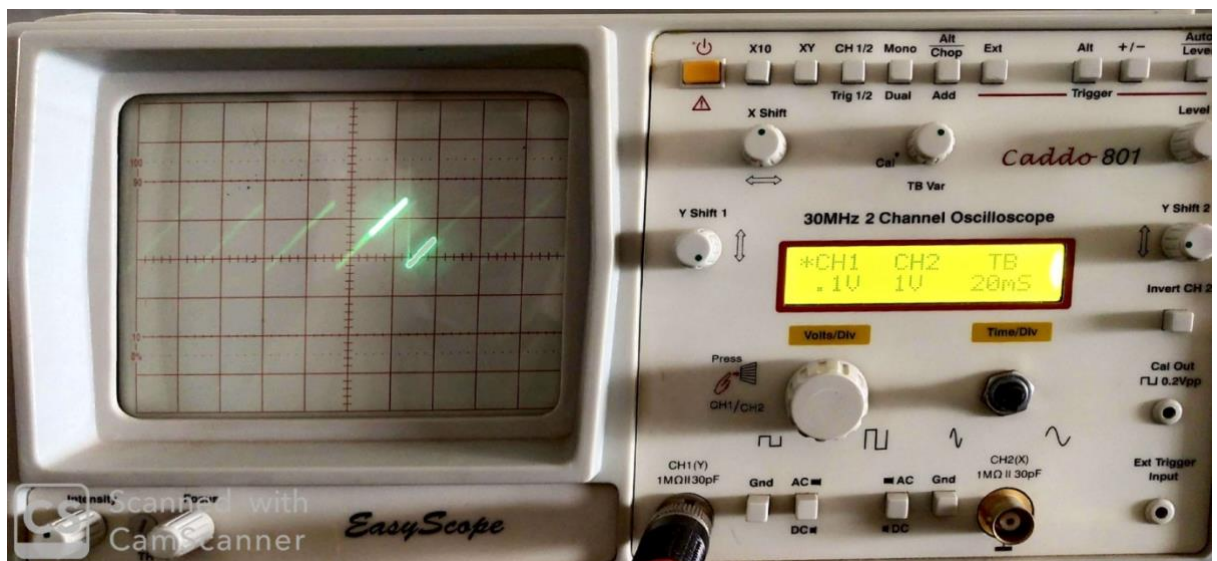


Figure 5.13:Wave form of triggering pulse of switch.

The figure 5.13 shows the waveform of triggering pulse of switch taken from CRO. Voltage= 2v,On-Time=14ms,Off-Time=1ms.



Figure 5.14: Waveform of output voltage across the switch.

Figure 5.14 shows the waveform of output voltage across the switch taken from CRO. Voltage =24v,On-Time=9.6ms,Off-Time=2.8ms.

CHAPTER 6

6.1 CONCLUSION

A single-stage high-frequency resonant ac/ac converter has been proposed in this project for a two-stage multichannel constant current ac/dc LED driver with high-frequency sinusoidal voltage bus. The performance of the converter was completely analyzed, including input power factor, voltage gain, THD of its output voltage, and the soft switching condition of the switches. A prototype was built and the experimental results have proven the correction of the theory analysis.

6.2 FUTURE SCOPE

Efficiency of the drives can be improved by improving the transformers performance in order to increase power density. An electrical converter can be used in order to convert the ac input to dc output so that the input to led drive can be given. The performance of the electrical converter can be improved by using high efficiency devices in order to drive the led. In order to have the good performance of the led drive the performance of the electrical converters and the output of the resonant converters can be improved.

We have to have LCL resonant rectifier.

CHAPTER 7

REFERENCES

1. A. Laubsch, M. Sabathil, J. Baur, M. Peter, and B. Hahn, “High-power and high-efficiency InGaN-based light emitters,” *IEEE Trans. Electron Devices*, vol. 57, no. 1, pp. 79–87, Jan. 2010.
2. H.-L. Cheng and C.-W. Lin, “Design and implementation of a high powerfactor LED driver with zero-voltage switching-on characteristics,” *IEEE Trans. Power Electron.*, vol. 29, no. 9, pp. 4949–4958, Sep. 2014.
3. C. S.Wong, K. H. Loo, Y. M. Lai, Martin H. L. Chow, and C. K. Tse, “An alternative approach to LED driver design based on high-voltage driving,” *IEEE Trans. Power Electron.*, vol. 31, no. 3, pp. 2465–2475, Mar. 2016.
4. R. A. Pinto, M. R. Cosetin, and A. Campos, M. A. Dalla Costa, and R. N.do Prado, “Compact emergency lamp using power LEDs,” *IEEE Trans. Ind. Electron.*, vol. 59, no. 4, pp. 1728–1738, Apr. 2012.
5. S. Y. R. Hui and Y. X.Qin, “A general photo-electro-thermal theory for light emitting diodes (LED) systems,” *IEEE Trans. Power Electron.*, vol. 24, no. 8, pp. 1967–1976, Aug. 2009.
6. Y. X. Qin and S. Y. R. Hui, “Comparative study on the structural designs of LED devices and systems based on the general photo-electrothermal theory,” *IEEE Trans. Power Electron.*, vol. 25, no. 6, pp. 507–513, Feb. 2010